



HAL
open science

Combined B–H and Si–H Bond Activations at Ruthenium

Ramaraj Ayyappan, Koushik Saha, Urminder Kaur, Sourav Gayen, Laure Vendier, Sylviane Sabo-Etienne, Sundargopal Ghosh, Sébastien Bontemps

► **To cite this version:**

Ramaraj Ayyappan, Koushik Saha, Urminder Kaur, Sourav Gayen, Laure Vendier, et al.. Combined B–H and Si–H Bond Activations at Ruthenium. *Organometallics*, 2023, 42 (9), pp.752-756. 10.1021/acs.organomet.3c00109 . hal-04169506

HAL Id: hal-04169506

<https://hal.science/hal-04169506v1>

Submitted on 24 Jul 2023

HAL is a multi-disciplinary open access archive for the deposit and dissemination of scientific research documents, whether they are published or not. The documents may come from teaching and research institutions in France or abroad, or from public or private research centers.

L'archive ouverte pluridisciplinaire **HAL**, est destinée au dépôt et à la diffusion de documents scientifiques de niveau recherche, publiés ou non, émanant des établissements d'enseignement et de recherche français ou étrangers, des laboratoires publics ou privés.

Combined B-H and Si-H bond activations at ruthenium

Ramaraj Ayyappan,^{a,‡} Koushik Saha,^b Urminder Kaur,^b Sourav Gayen,^b Laure Vendier,^a Sylviane Sabo-Etienne,^a Sundargopal Ghosh,^{*b} Sébastien Bontemps^{*a}

^a LCC-CNRS, Université de Toulouse, CNRS, 205 route de Narbonne, 31077 Toulouse Cedex 04, France.

^b Department of Chemistry, Indian Institute of Technology Madras, Chennai 600036, India.

[‡] Present address: Indian Institute of Science Education and Research Thiruvananthapuram (IISER-TVM), Maruthamala PO, Vithura, Thiruvananthapuram - 695551. Kerala, India

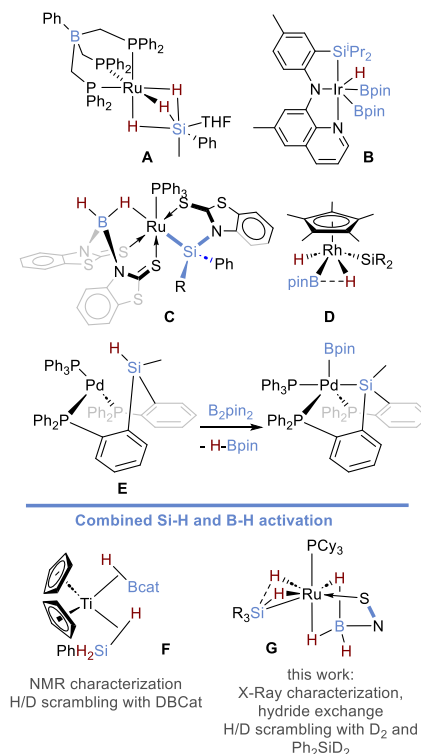
ABSTRACT: The coordination of 2-mercaptobenzothiazolyl (mbz) and 2-mercaptopyridyl (mp) to a [Ru]-H precursor led to the isolation of two hydrido(dihydroborate) complexes [RuH(PCy₃)₂{κ³-H,H,S-(H)₂BH(L)}] (L = mbz (**1a**), mp (**1b**)). Oxidative addition of secondary and tertiary silanes to **1a** and **1b** afforded the dihydrido ruthenium(IV) [RuH₂(SiPh₂R)(PCy₃)₂{κ³-H,H,S-(H)₂BH(L)}] (R = H, L = mbz (**2a**), mp (**2b**); R = Me, L = mbz (**2c**)) featuring a coordinated borohydride moiety and a silyl ligand in weak interaction with the two hydride ligands of the ruthenium center. 1D and 2D NMR investigations at different temperatures as well as D₂ reactivity enabled to characterize exchange between every Si-H, Ru-H and B-H hydride sites.

The coordination chemistry of Si-H or B-H bonds toward metal centers has been the subject of a multitude of investigations aiming at characterizing every step of E-H bond activation (E = B or Si) from the weakest interactions to the ultimate breaking of the bond at a metal center (M) with or without the assistance of a co-ligand.¹⁻¹⁰ These studies fueled the knowledge and comparisons on reduction and functionalization reactions by boranes or silanes both in stoichiometric and catalytic conditions.

However, the combination of both boron and silicon, and hydrides in the coordination sphere of a metal center is much rarer. We have selected representative examples in Scheme 1. Complexes **A-D** exhibit such specific features. The tris(diphenylphosphinomethyl)borato ligand in complex **A** is an example of ligand featuring an anionic charge in the backbone, with a borate moiety. Complex **A** shows that such ligand can support a Ru center able to activate silanes (RR'SiH₂).¹¹ Complex **B** was used in dehydrogenative borylation of alkynes¹² and complex **C** is the result of silane activation at Ru bearing a di(mercaptobenzothiazolyl)borate ligand.¹³ Complex **D** features a boryl, silyl and two hydride ligands at a single Rh center. Remaining H...Bpin interaction was evidenced in solid-state by short contact in the X-ray diffraction analysis and in solution by B-H coupling observed in ¹H NMR analysis. This complex was shown to release hydroborane and not hydrosilane upon thermic activation.¹⁴ Finally, complex **E** was reacted with B₂pin₂ to generate two isomeric boryl complexes differing by the relative positioning of the boryl and silyl moieties (cis-B,Si, shown in Scheme 1 and trans-B,Si, not drawn).¹⁵ Theoretical investigation proposed that these boryl complexes were generated via Si-H and B-H activation.

To our knowledge, the combined activation of Si-H and B-H bond has only been studied once at a Ti center (complex **F**, Scheme 1) with hydrosilane (PhSiH₃) and hydroborane (H-BCat) ligands.¹⁶ The archetypal bisboranetitanocene complex [Cp₂Ti(HBCat)₂]¹⁷ was reacted with phenylsilane resulting in

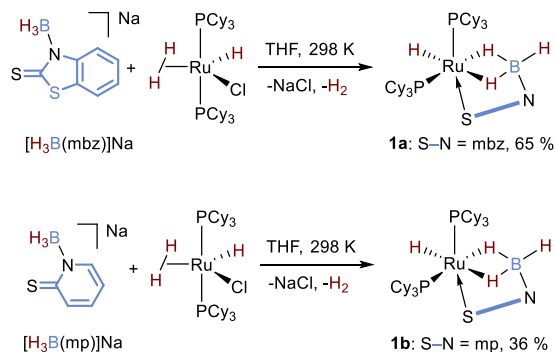
the formation of the σ-silane-σ-borane titanocene complex **F**. The relative orientation of both sigma ligands was determined by NOESY NMR investigation. Hydride exchange was evidenced by the reaction of [Cp₂Ti(DBCat)₂] with phenylsilane resulting in the partial deuteration of the phenylsilane ligand. A silyldihydroborate intermediate was proposed to explain this H/D scrambling.



Scheme 1. Relevant examples of complexes featuring both Si and B elements around a metal center.

The use of BH₃ adducts of 2-mercaptobenzothiazolyl (mbz) and 2-mercaptopyridyl (mp) in coordination chemistry led to the isolation of a variety of new structures featuring a hydroborate ligand with different transition metal centers.¹⁸ Notable examples are [Cp**Ru*(CO)(κ²-H, S)BH₂(mbz)] and [Rh{κ³-H,H,S-(H)₂BH(mp)}(NBD)] complexes involving Ru–H–B bond in hydroboration reaction.^{19–20} Using these ligands, we wished to explore the combined presence of Si–H and B–H bonds at a metal center with a 4-coordinate boron moiety. In the present work, oxidative addition of hydrosilanes (Ph₂(R)Si–H) is described with [RuH(PCy₃)₂{κ³-H,H,S-(H)₂BH₃(L)}] (L = mbz or mp) complexes. In-depth multinuclear NMR and D₂ scrambling established the H/D exchange between B–H and Si–H and Ru–H moieties.

Treatment of [RuH(H₂)Cl(PCy₃)₂] with mono-substituted trihydroborate ligands Na[H₃B(L)] (L = mbz, mp) resulted in the formation of ruthenium dihydridoborate complexes **1a** and **1b**, isolated in good yields as a yellow and red powder, respectively (Scheme 2). The spectral features gathered from NMR for **1a** and **1b** (Table S1) and X-Ray diffraction analysis for **1b** indicate a facial arrangement of the H₃B(L) ligand {κ³-H,H,S} where two of the σ(B–H) bonds of the BH₃ unit and the sulphur atom of the heterocycle coordinate with the ruthenium. One phosphine ligand is in axial position while the other is in the equatorial plane completed by a hydride ligand. Both complexes exhibit similar spectral characteristics. Key NMR parameters of **1a** are highlighted here. The Ru–H resonates at δ –11.98, as a doublet of doublet due to cis interaction with the two phosphines (²J_{H–P} of 35.4 and 26.8 Hz) in the ¹H NMR spectrum. The three B–H signals appear distinctively: the two Ru–H–B signals at δ –9.72 (d, ²J_{H–P} = 36.3 Hz) and –4.57 (br s) while the terminal B–H resonates at δ 4.86 as detected by ¹H{¹¹B} NMR analysis. The relative arrangement of the hydride and B–H hydrogens around ruthenium was identified using selective decoupling ¹H{¹¹B} and ¹H-³¹P{¹H} HMQC experiments. The ³¹P{¹H} NMR spectrum reveals an AX pattern with the presence of two doublets at δ 69.4 and 57.8 with cis ²J_{P–P} of 21.3 Hz, while the ¹¹B{¹H} NMR spectrum reveals a singlet at δ 11.7.



Scheme 2. Synthesis of ruthenium (II) dihydridoborate complexes 1a and 1b complexes 1a and 1b.

In the solid-state IR spectrum, the B–H and Ru–H stretching frequencies were respectively identified at 2461 and 1990 cm⁻¹ for **1a** and at 2436 and 1959 cm⁻¹ for **1b**. Monocrystals of **1b** suitable for X-ray diffraction analysis were obtained from a saturated Et₂O solution at 213 K. In accordance with NMR study in solution, the X-ray diffraction analysis revealed a distorted octahedral geometry containing facial arrangement of the {H₃B(mp)} ligand around the ruthenium center (Figure 1). The two phosphines are cis to one another with ∠P–Ru–P =

105.89(4)°. The Ru–P2 distance of 2.3052(10) Å is shorter compared to the Ru–P1 distance 2.3254(11) Å due to the different trans donor ligands (BH vs S) and the difference between equatorial and axial site occupancy. The Ru–B separation of 2.225(5) Å in **1b** is comparable to those of dihydridoborate complexes such as [Cp**Ru*{κ³-H,H,S-(H)₂BH(mbz)}] (2.216(6) Å), and [RuH{(μ-H)₂BMeCH₂SMe}(PCy₃)₂] (2.266(8) Å) and smaller than the sum of their covalent radii (2.30 Å).²¹ The alternating carbon-carbon bond distances in pyridine ring suggest the presence of dearomatized pyridine ring containing 2-thione donor (C1–S1 1.692(4) Å).²² The bond distances discussed here compare well with the DFT optimized structure of **1b** (Table S7) enabling to ascertain the location of the hydride atoms.

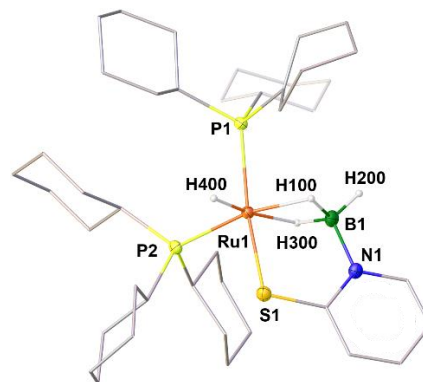
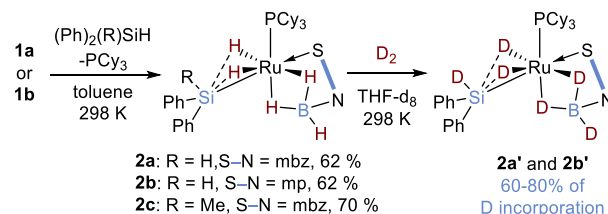


Figure 1. Solid-state molecular structure of **1b**. Partial thermal ellipsoids were drawn at 75% probability. Ru–H and B–H hydrogen atoms were located in the difference Fourier map and isotropically refined. Ellipsoids of all the carbon atoms and the hydrogen atoms associated with the carbon atoms were omitted for clarity. Selected bond lengths (Å): Ru1–B1 2.225(5), Ru1–P1 2.3254(11), Ru1–P2 2.3052(10), B1–N1 1.540(6), Ru1–S1 2.3516(11), Ru1–H300 1.82(4), Ru1–H100 1.78(3), Ru1–H400 1.51(4).

Hydrido complexes **1a** and **1b** were reacted with secondary and tertiary silanes. The reactions of **1a** and **1b** with Ph₂SiH₂ led to the formal oxidative addition of the Si–H bond and the displacement of one PCy₃ ligand. The resulting ruthenium (IV) silyl dihydride complexes [RuH₂(SiPh₂H)(PCy₃)-{κ³-H,H,S-(H)₂BH(L)}] (L = mbz (**2a**), mp (**2b**)) are shown in Scheme 3. Similarly, complex **2c** [RuH₂(SiPh₂Me)(PCy₃){κ³-H,H,S-(H)₂BH(mbz)}] was synthesized by the reaction of **1a** with Ph₂MeSiH (Scheme 3).



Scheme 3. Synthesis of the silyl ruthenium (IV) dihydridoborate complexes 2a-c and reactivity toward D₂.

We decided to probe the unique presence of several types of hydrides in these complexes by means of NMR studies and deuteration experiments. NMR spectral characteristics of **2a**, **2b** and **2c** are similar. Key NMR parameters of **2a** are highlighted here. The P and B nuclei were characterized at δ 74.0 and 12.5, respectively, close to the corresponding signals of **1a**. In the ²⁹Si{¹H} NMR spectrum, a singlet is noted at δ 5.7 indicating

the formation of a silyl ligand. Figure 2 shows ^1H NMR (Figure 2a), 1D HSQC ^1H (Figure 2b) and 1D HSQC ^1H analyses, with several selective decoupling (Figure 2c-e). While only $J_{\text{P-H}}$ coupling is apparent on the ^1H NMR spectrum (Figure 2a), the selective 1D HSQC $^1\text{H}\{^{31}\text{P}\}$ experiments (Figure 2c) provided $J_{\text{Si-H}}$ of 12 Hz, supporting weak secondary interactions between silicon and ruthenium hydrides. The Ru-H \cdots Si hypervalent interactions were also characterized by 2D ^1H - ^{29}Si HMQC experiments.

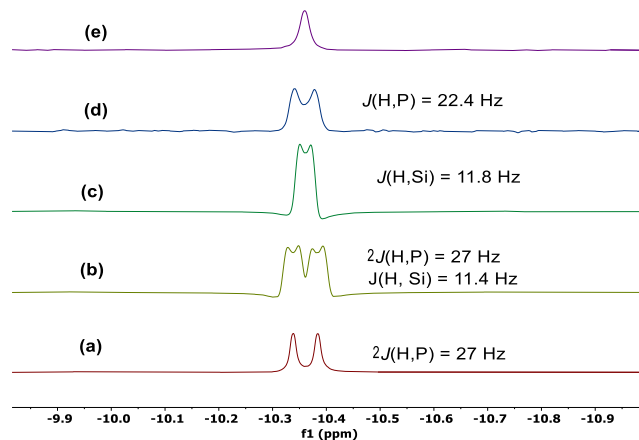


Figure 2. Selective 1D ^1H HSQC NMR spectral stack plot of **2a** in $\text{tol-}d_8$ at 298 K. (a) ^1H , (b) 1D HSQC selective ^1H , (c) $^1\text{H}\{^{31}\text{P}\}$, (d) $^1\text{H}\{^{29}\text{Si}\}$ and (e) $^1\text{H}\{^{31}\text{P}\}\{^{29}\text{Si}\}$.

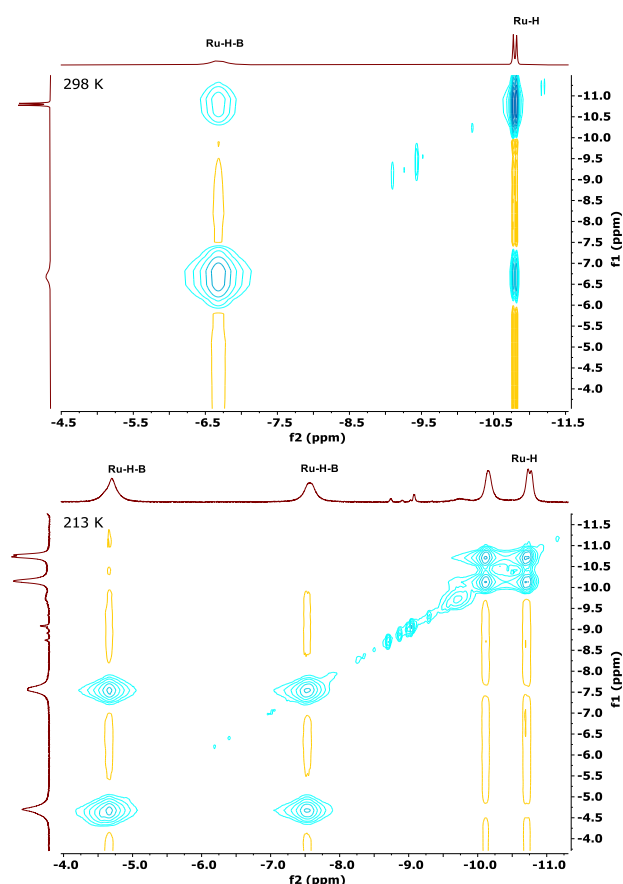


Figure 3. EXSY NMR analyses of Ru-H and Ru-H-B of **2a** at 298 K (top) and 213 K (bottom). (600.47 MHz, $d_1 = 1.5$ s, mixing time 0.05 s)

At 273 K, the terminal Si-H and B-H appear at δ 6.10 and 5.29, respectively. At this temperature, the two hydrides bonded to Ru (Ru-H) and the two hydrides bridging Ru and B (Ru-H-B) appear equivalent at δ -10.40 and -6.27, respectively (traces in Figure 3 top taken at 298 K). When lowering the temperature to 213 K, the two signals of Ru-H and Ru-H-B resolved to four signals at δ -10.75 (d, $^2J_{\text{H-P}}$ 32.6 Hz), -10.15 (s) for the two Ru-H, and at δ -7.57 (s) and -4.70 (s) for the two Ru-H-B. (traces Figure 3, bottom). The integral ratio of these four signals is identical (1:1:1:1). EXSY NMR experiments were then conducted to assess the exchange between the different hydrides (Figure 3). The Ru-H and Ru-H-B hydrides are in exchange at 298 K, (Figure 3, top) but frozen at 213 K. At this lower temperature, the hydrides of same type are still exchanging since cross-linked correlations are observed between the two Ru-H on one hand and the two Ru-H-B on the other hand (Figure 3, bottom).

In the solid-state IR spectrum of **2a**, Ru-H-B and Ru-H stretching frequencies are measured at 2502, and 2077, 1971 cm^{-1} respectively. Monocrystals suitable for X-ray diffraction analysis were obtained by layering toluene solution of **2a** or **2c** with n-pentane at -35°C . The solid-state molecular structures are shown in Figure 4. The B-H and Ru-H hydrogens of **2a** and **2c** were located in the Fourier map and refined isotropically. The Ru-Si bond distances are of 2.3538(6) and 2.3575(6) Å respectively for **2a** and **2c** and within the range of Ru-SiR₃ complexes (Table S3). Si \cdots H-Ru distances of 2.183 and 1.941 Å were measured for **2a** and of 2.001 and 2.063 Å for **2c**. These distances are shorter than the sum of Van der Waals radii of silicon and hydrogen (3.4 Å) and correspond to secondary interactions between silicon and hydrogen atoms (SISHA) (1.9-2.4 Å), in line with small $J_{\text{Si-H}}$ observed in solution.²³ These interactions arise from the electrophilicity and hypervalency of the silicon atom and have been shown to be crucial catalytic intermediates.²⁴ The silicon atoms are out of the equatorial planes with Si-Ru-H acute angles (74.4(10) $^\circ$, 63.8(10) $^\circ$ for **2a**; 59.8(8) $^\circ$, 57.3(9) $^\circ$ for **2c**) in a distorted capped octahedral geometry²⁵⁻²⁶ differing from other possible geometries encountered in Ru(silylhydride) complexes.²⁷⁻²⁸ The bridging Ru-H-B distances are significantly longer 1.771, 1.823 Å as compared to the terminal Ru-H distances 1.640 and 1.593 Å. Similarly, the terminal B-H distance (1.018 Å) is shorter as compared to bridging Ru-H-B distances (1.224 and 1.286 Å). The geometrical parameters in the optimized structures of **2a** and **2c** are in good agreement with X-ray data (Table S7), and highlight the presence of secondary Si \cdots H-Ru interactions in the range of 1.941-2.183 Å. According to our calculations, NPA charges of Ru-H200 and Ru-H400 in **2a** are notably more positive than the related Ru-H in **1a**.

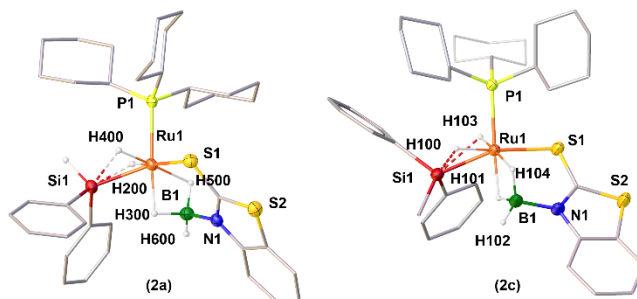


Figure 4. Solid-state molecular structures of **2a** and **2c**. Si-H, Ru-H and B-H hydrogen atoms were located in the difference Fourier map and isotropically refined. Partial thermal ellipsoids were

drawn at 75% probability. Ellipsoids of all the carbon atoms and the hydrogen atoms associated with the carbon atoms were omitted for clarity. The dotted lines represent secondary Si...H–Ru interactions. Selected bond lengths (Å): **2a**: B1–N1 1.520(3), Ru1–P1 2.3007(5), Ru1–B1 2.221(2), Ru1–Si1 2.3538(6), Ru1–S1 2.3837(6), Ru1–H300 1.77(3), Ru1–H500 1.83(2), Ru1–H200 1.64(3), Ru1–H400 1.59(3); **2c**: Ru1–B1 2.224(2), Ru1–P1 2.3173(5), B1–N1 1.533(3), Ru1–S1 2.3838(5), Ru1–Si1 2.3575(6), Ru1–H100 1.54(2), Ru1–H101 1.71(3), Ru1–H104 1.82(3), Ru1–H103 1.51(3).

To explore further the dynamics of the different hydrides, complexes **2a** and **2b** were exposed to 3 atm of D₂ in THF-d₈ at 298 K (Scheme 3). Deuterium incorporation was observed at the Ru–H–B and Ru–H sites, by the disappearance of the signals in ¹H NMR and the appearance of deuteride signals in ²H NMR spectroscopy (ESI). The formations of free H–D (δ 4.51) and H₂ (δ 4.54) were noted in the ¹H NMR spectrum. For **2a**, after 3 weeks, a maximum deuteration level of 59% and 64% had been reached for Ru–H and Ru–H–B sites, respectively. Moreover, 78% and 69% deuteration of SiHPh₂ and terminal B–H hydrogens was also observed respectively. The formation of isotopomers was also reflected in the ³¹P{¹H} NMR spectroscopy where the signals were slightly downfield shifted. H/D exchange for every hydride was also observed by reacting **1a** with D₂SiPh₂, which generated **2a'** within 3 days at room temperature. Similar observations were made for the reactivity of **2b** toward D₂ and for the reactivity of **1b** with D₂SiPh₂.

In conclusion, the synthesis of Ruthenium (II) dihydridoborate complexes **1a–1b**, led to the generation of ruthenium (IV) silyl dihydride complexes **2a–2c**. The silyl ligand features weak secondary silicon hydrogen interactions (Si...H–Ru, 1.941–2.183 Å) which were characterized by NMR spectroscopy, X-ray diffraction analysis and DFT calculations. These complexes are unique because they exhibit a rare combination of boron, silicon and hydride elements around a single metal center. The present study proved that all hydrides are in exchange in the NMR time scale and undergo scrambling with D₂(g). This was characterized by EXSY and ²H NMR spectroscopy. This study showed that in these new complexes, Si–H bond activation can occur while preserving the dihydroborate ligand. It will be interesting to perform additional reactivity and catalytic studies to evaluate the competition between Si–H and B–H bond activation.

ASSOCIATED CONTENT

Supporting Information

The Supporting Information is available free of charge on the ACS Publications website. It includes experimental details, compounds synthesis and characterization.

AUTHOR INFORMATION

Corresponding Author

Sundargopal Ghosh, sghosh@iitm.ac.in,
Sébastien Bontemps sebastien.bontemps@lcc-toulouse.fr

ACKNOWLEDGMENT

We gratefully acknowledge financial support from CNRS and CEFIPRA on project 5905-1. C. Bijani and Y. Coppel are warmly acknowledge for their insights in NMR investigations. U.K. and S.G. thanks IIT Madras and CSIR India, respectively for their research fellowships.

NOTE

"The authors declare no competing financial interests."

REFERENCES

- Geier, S. J.; Vogels, C. M.; Melanson, J. A.; Westcott, S. A.; The transition metal-catalysed hydroboration reaction, *Chem. Soc. Rev.* **2022**, *51*, 8877.
- Saha, K.; Roy, D. K.; Dewhurst, R. D.; Ghosh, S.; Braunschweig, H.; Recent Advances in the Synthesis and Reactivity of Transition Metal σ-Borane/Borate Complexes, *Acc. Chem. Res.* **2021**, *54*, 1260.
- Corey, J. Y.; Reactions of Hydrosilanes with Transition Metal Complexes, *Chem. Rev.* **2016**, *116*, 11291.
- Corey, J. Y.; Reactions of Hydrosilanes with Transition Metal Complexes and Characterization of the Products, *Chem. Rev.* **2011**, *111*, 863.
- Corey, J. Y.; Braddock-Wilking, J.; Reactions of Hydrosilanes with Transition-Metal Complexes: Formation of Stable Transition-Metal Silyl Compounds, *Chem. Rev.* **1999**, *99*, 175.
- Perutz, R. N.; Sabo-Etienne, S.; Weller, A. S.; Metathesis by Partner Interchange in σ-Bond Ligands: Expanding Applications of the σ-CAM Mechanism, *Angew. Chem. Int. Ed.* **2022**, *61*, e202111462.
- Perutz, R. N.; Sabo-Etienne, S.; The σ-CAM mechanism: s complexes as the basis of σ-bond metathesis at late-transition-metal centers, *Angew. Chem. Int. Ed.* **2007**, *46*, 2578.
- Cheng, C.; Hartwig, J. F.; Catalytic Silylation of Unactivated C–H Bonds, *Chem. Rev.* **2015**, *115*, 8946.
- Hartwig, J. F.; Borylation and Silylation of C–H Bonds: A Platform for Diverse C–H Bond Functionalizations, *Acc. Chem. Res.* **2011**, *45*, 864.
- Mkhalid, I. A. I.; Barnard, J. H.; Marder, T. B.; Murphy, J. M.; Hartwig, J. F.; C–H Activation for the Construction of C–B Bonds, *Chem. Rev.* **2010**, *110*, 890.
- Lipke, M. C.; Tilley, T. D.; High Electrophilicity at Silicon in η³-Silane σ-Complexes: Lewis Base Adducts of a Silane Ligand, Featuring Octahedral Silicon and Three Ru–H–Si Interactions, *J. Am. Chem. Soc.* **2011**, *133*, 16374.
- Lee, C.-I.; Zhou, J.; Ozerov, O. V.; Catalytic Dehydrogenative Borylation of Terminal Alkynes by a SiNN Pincer Complex of Iridium, *J. Am. Chem. Soc.* **2013**, *135*, 3560.
- Zafar, M.; Ramalakshmi, R.; Ahmad, A.; Antharjanam, P. K. S.; Bontemps, S.; Sabo-Etienne, S.; Ghosh, S.; Cooperative B–H and Si–H Bond Activations by κ²-N,S-Chelated Ruthenium Borate Complexes, *Inorg. Chem.* **2021**, *60*, 1183.
- Cook, K. S.; Incarvito, C. D.; Webster, C. E.; Fan, Y.; Hall, M. B.; Hartwig, J. F.; Rhodium Silyl Boryl Hydride Complexes: Comparison of Bonding and the Rates of Elimination of Borane, Silane, and Dihydrogen, *Angew. Chem. Int. Ed.* **2004**, *43*, 5474.
- Kirai, N.; Takaya, J.; Iwasawa, N.; Two Reversible σ-Bond Metathesis Pathways for Boron–Palladium Bond Formation: Selective Synthesis of Isomeric Five-Coordinate Borylpalladium Complexes, *J. Am. Chem. Soc.* **2013**, *135*, 2493.
- Muhoro, C. N.; He, X.; Hartwig, J. F.; Titanocene Borane σ-Complexes, *J. Am. Chem. Soc.* **1999**, *121*, 5033.
- Hartwig, J. F.; Muhoro, C. N.; He, X.; Eisenstein, O.; Bosque, R.; Maseras, F.; Catecholborane Bound to Titanocene. Unusual Coordination of Ligand s-Bonds, *J. Am. Chem. Soc.* **1996**, *118*, 10936.
- Saha, K.; Ghosh, S.; Hydroboration reactions using transition metal borane and borate complexes: an overview, *Dalton Trans.* **2022**, *51*, 2631.
- Iannetelli, A.; Tizzard, G.; Coles, S. J.; Owen, G. R.; Sequential Migrations between Boron and Rhodium Centers: A

Cooperative Process between Rhodium and a Monosubstituted Borohydride Unit, *Inorg. Chem.* **2018**, *57*, 446.

20. Saha, K.; Joseph, B.; Ramalakshmi, R.; Anju, R. S.; Varghese, B.; Ghosh, S.; η^4 -HBCC- σ,π -Borataallyl Complexes of Ruthenium Comprising an Agostic Interaction, *Chem. Eur. J.* **2016**, *22*, 7871.

21. Cordero, B.; Gómez, V.; Platero-Prats, A. E.; Revés, M.; Echeverría, J.; Cremades, E.; Barragán, F.; Alvarez, S.; Covalent radii revisited, *Dalton Trans.* **2008**, 2832.

22. Gloaguen, Y.; Alcaraz, G.; Pécharman, A.-F.; Clot, E.; Vendier, L.; Sabo-Etienne, S.; Phosphinoborane and Sulfidoborohydride as Chelating Ligands in Polyhydride Ruthenium Complexes: Agostic sigma-Borane versus Dihydroborate Coordination, *Angew. Chem. Int. Ed.* **2009**, *48*, 2964.

23. Lachaize, S.; Sabo-Etienne, S.; σ -Silane ruthenium complexes: the crucial role of secondary interactions, *Eur. J. Inorg. Chem.* **2006**, 2115.

24. Alcaraz, G.; Sabo-Etienne, S.; NMR: A good tool to ascertain σ -silane or σ -borane formulations?, *Coord. Chem. Rev.* **2008**, *252*, 2395.

25. Eguillor, B.; Esteruelas, M. A.; Lezáun, V.; Oliván, M.; Oñate, E.; Tsai, J.-Y.; Xia, C.; A Capped Octahedral MHC6 Compound of a Platinum Group Metal, *Chem. Eur. J.* **2016**, *22*, 9106.

26. Esteruelas, M. A.; Oñate, E.; Palacios, A.; Tsai, J.-Y.; Xia, C.; Preparation of Capped Octahedral OsHC₆ Complexes by Sequential Carbon-Directed C–H Bond Activation Reactions, *Organometallics* **2016**, *35*, 2532.

27. Dioumaev, V. K.; Procopio, L. J.; Carroll, P. J.; Berry, D. H.; Synthesis and Reactivity of Silyl Ruthenium Complexes: The Importance of Trans Effects in C–H Activation, Si–C Bond Formation, and Dehydrogenative Coupling of Silanes, *J. Am. Chem. Soc.* **2003**, *125*, 8043.

28. Dioumaev, V. K.; Yoo, B. R.; Procopio, L. J.; Carroll, P. J.; Berry, D. H.; Structure and Reactivity of Bis(silyl) Dihydride Complexes (PMe₃)₃Ru(SiR₃)₂(H)₂: Model Compounds and Real Intermediates in a Dehydrogenative C–Si Bond Forming Reaction, *J. Am. Chem. Soc.* **2003**, *125*, 8936.

Oxidative addition of diphenyl- and methylphenyl-silanes onto ruthenium-borate complexes **1a-b** afforded **2a-c** featuring four different hydrogens bonded to the ruthenium. EXSY and H/D scrambling studies showed the rapid exchange between the Ru–H \cdots Si and Ru–H–B hydrogens at 298 K.

